Proceedings of the 14th International Conference on Cyclotrons and their Applications, Cape Town, South Africa

A NUMERICAL STUDY OF THE SPACE CHARGE EFFECTS IN A SPIRAL INFLECTOR

M. SEKIGUCHI

Institute for Nuclear Study, University of Tokyo, 3-2-1 Midori-cho, Tanashi-shi, Tokyo 188, Japan

Computer simulations have been carried out to find out numerically the effects of the space charge on the optical properties of the spiral inflector. The electric field due to the space charge was introduced in an approximate way: the potential produced by an infinitely long uniformly charged line. It was found that 1) transmission and its beam current dependence strongly depend on the type of the inflectors and their parameters, and 2) the space charge have considerable effects on the transmission for some type of inflector when the intensity exceeds a few mA in the case of Ar^{10+} at 10 kV.

1 Introduction

A spiral inflector is a device to deflect ions entering it along the main magnetic field of the cyclotron into the direction perpendicular to the field at its exit, by means of an electric field perpendicular to the ion velocity all through the passage. Although it is a small component of the cyclotron, it becomes more important as more powerful external ion sources are used for cyclotrons and more intense beams are supplied from the sources.

It is reasonable to expect that when the beam intensity becomes high enough, the optical properties of the inflector would be affected by the space charge force of the beam because of the following reasons: 1) the velocity of the ions to be deflected is generally low, and 2) the space for the inflector is limited in a narrow region of the cyclotron center and the beam is inevitably focussed into a small size by the effect of the solenoidal magnetic field.

A formulation of the orbit through the spiral inflector was presented before, [1] which can treat all types of the inflectors in a general way and enables one to study and design spiral inflectors in a simple and transparent way. Although it does not include the effects of deformation of the electric field at the electrode edges, it can be applied to study the effects of the space charge of the beam on the optical properties approximately, since it separates the motion in longitudinal and transverse directions and uses the electric potential in the transverse plane while taking the twisting of the orbit into account.

In this paper, results of numerical studies based upon this formulation are presented to study the possible effects of the space charge.

2 Review of the Formulation

Since the formulation was presented in some detail before, only the essential points are reviewed to introduce the concept and notations.

2.1 Central trajectory

The central trajectory is considered to be a three-dimensional curve defined by three mutually orthogonal unit vectors ($\boldsymbol{e}$, $\boldsymbol{n}$, $\boldsymbol{t}$), where $\boldsymbol{t}$ is the tangent to the curve. These vectors are solution of three simultaneous differential equations with respect to the distance along the trajectory s from the entrance, one of which is the equation of motion of the reference ion. They include the electric curvature functions of s, K and F, an auxiliary function G and the magnetic curvature vector $\boldsymbol{b}$. The fields are given by

$$\boldsymbol{B} = \frac{mv}{e}\boldsymbol{b} \tag{1}$$

and

$$\boldsymbol{E} = \frac{mv^2}{e}\left(K\boldsymbol{e} - F\boldsymbol{n}\right), \tag{2}$$

where m, e and v are the mass, charge and the velocity of the ion, respectively. The radius vector $\boldsymbol{r}_C(\boldsymbol{s})$ can be obtained by integrating $\boldsymbol{t}$ with respect to s with appropriate initial conditions.

In the case of the uniform magnetic field, where $\boldsymbol{B} = (0, 0, B)$, $B = \mathrm{const}$, it has been shown that they have simple solutions with

$$K = C_e, F = C_f \sin\alpha, G = -C_f \cos\alpha \tag{3}$$

and

$$\alpha = C_e s + \alpha_0, \tag{4}$$

where C_e, C_f and α_0 are constants characterizing the electric field. The strength of the electric field is given by

$$E = 2V_i\left\{C_e^2 + C_f^2\sin^2(C_e s + \alpha_0)\right\}^{1/2}, \tag{5}$$

where V_i is the injection voltage. Thus the central trajectory is characterized completely by two electric radii of curvature, $R_e = 1/C_e$ and $R_f = 1/C_f$ and a phase angle α_0, in addition to the magnetic radius of curvature, $R_m = 1/C_m$.

The solution contains only trigonometric functions and includes all of the inflector types:

normal [2] : $C_e \neq 0,\ C_f = 0,\ \alpha_0 = 0$
slanted [2] : $C_e \neq 0,\ C_f \neq 0,\ \alpha_0 = 0$
hyperboloid [3] : $C_e = C_m/\sqrt{6},\ C_f = -C_m/2,\ \alpha_0 = 0$
paraboloid [3] : $C_e = C_m/2,\ C_f = -C_m/2,\ \alpha_0 = 0$
parallel [1] : $C_e = 0,\ C_f \neq 0,\ \alpha_0 \neq 0$.

It should be noted that the strength of the electric field is constant along the trajectory only when $C_e C_f = 0$. In other words, the gap between the electrodes decreases in the cases of *slanted, hyperboloid* and *paraboloid*. This situation naturally affects the transmission efficiency of the beam.

2.2 Non-central trajectories

The equation of motion is transformed from a Cartesian coordinate into a curvilinear coordinate (ξ, η, s), whose reference curve is the central trajectory:

$$\boldsymbol{r}(\xi, \eta, s) = \boldsymbol{r}_C(s) + \xi \boldsymbol{e}(s) + \eta \boldsymbol{n}(s), \tag{6}$$

by introducing a radius vector

$$\boldsymbol{q} = \boldsymbol{r} - \boldsymbol{r}_C \tag{7}$$

in the transverse plane $\boldsymbol{q} \cdot \boldsymbol{t} = 0$, and a vector

$$\boldsymbol{p} = \frac{d\boldsymbol{r}}{du} - \boldsymbol{t}, \tag{8}$$

which describes the difference of the ion velocity with respect to the reference one. The quantity u has a dimension of length, $u = vt$, where t is the time elapsed after entering the inflector. The transformed equations are

$$\boldsymbol{q}' = u'\boldsymbol{p} + (u' - 1)\boldsymbol{t} \tag{9}$$

for the radius vector and

$$\begin{aligned} \boldsymbol{p}' &= (u' - 1)\{\boldsymbol{C}_C + [\boldsymbol{t} \times \boldsymbol{b}_C]\} \\ &\quad + u'(\boldsymbol{C} - \boldsymbol{C}_C) + u'[\boldsymbol{p} \times \boldsymbol{b}_C] \end{aligned} \tag{10}$$

for the vector $\boldsymbol{p}$ in the case of the uniform field with a subsidiary condition

$$u' = \frac{\lambda}{1 + \boldsymbol{p} \cdot \boldsymbol{t}} \tag{11}$$

$$\lambda = 1 - a\xi + b\eta, . \tag{12}$$

where $a = (\boldsymbol{e} \cdot \boldsymbol{t}')$ and $b = (\boldsymbol{n}' \cdot \boldsymbol{t})$, and the primes designate differentiation with respect to s.

These equations can be solved numerically, if we know the electric curvature vector

$$\boldsymbol{C}_C = K\boldsymbol{e} - F\boldsymbol{n} = C_e \boldsymbol{e} - (C_f \sin\alpha)\boldsymbol{n} \tag{13}$$

and

$$\boldsymbol{C} = C_e \boldsymbol{e} + C_n \boldsymbol{n} + C_t \boldsymbol{t}. \tag{14}$$

2.3 Potential expansion

It is necessary to know the electric potential around the central trajectory in order to calculate the optical properties of an inflector. Since the electric field is given on the central trajectory it is more convenient to expand the electric potential around it, rather than to solve boundary value problem.

A method was devised to expand the electric potential in terms of a polynomial of ξ and η, which satisfies the Laplace equation to a given order around a three dimensional curve. This method itself is independent from the inflector problem discussed here and can be applied to any problem. If two electrodes are set on the equipotential surface of the resultant polynomial, the assumed electric field is obtained on the reference curve.

Two of such polynomials relevant to the discussions here are:

$$\phi_\xi = k\xi + \frac{ka}{4}(\xi^2 + \eta^2) + \ldots \tag{15}$$

and

$$\phi_\eta = f\eta - \frac{fb}{4}(\xi^2 + \eta^2) + \ldots, \tag{16}$$

which tend to a parallel plate deflector in ξ and η directions when the twisting of the reference curve goes to zero. The strength functions k and f are generally functions of s, but in the present application to the inflector, we can identify $k = C_e$, and $f = -C_f \sin\alpha$. Note that ϕ's are normalized by $2V_i$. Any linear combination of these functions satisfies also the Laplace equation to the same order.

The accuracy of the polynomial expansion can be checked in two ways: 1) by comparing the potential with the known solution of *hyperoloid* type and 2) by calculating the residue of the Laplacian from the obtained polynomial:

$$\Delta\phi = \delta. \tag{17}$$

The concrete expression for δ can be obtained as the residue of the Laplacian in the course of expansion and numerical values will be discussed in the next section.

3 Optical Properties without Space Charge

In order to study the optical properties of the inflector and clarify the various aspects of the inflector optics numerically, let us introduce models of the inflector together with simplifying assumptions on the cyclotron. A variable-energy cyclotron with a 180° single-dee at a dee voltage V_d = 50 kV, operated in a constant orbit mode with number of turns N = 250 up to the extraction radius, R_{ext} = 730 mm, is assumed. We assume a constant magnetic field for simplicity. Thus, if we define $R_0 = R_{ext}/\sqrt{2N + K_i} \approx R_{ext}/\sqrt{2N}$, then $K_i = V_i/V_d$ and $R_m = \sqrt{K_i}R_0$.

Table 1: Numerical values of various parameters for the selected models. R_0 = 32.7 mm, V_d = 50 kV, $V_i = K_i V_d$. N6:*normal*, S6:*slanted*, H6:*hyperboloid*, P6a, P6b:*parallel*. E_i and E_f are the strength of the electric field at the entrance and exit.

	N6	S6	H6	P6a	P6b
R_e (mm)	38.2	38.2	38.2	0	0
R_f (mm)	0	38.2	-31.2	31.4	31.4
α_0 (deg)	0	0	0	60	120
K_i	0.285	0.761	0.229	0.464	0.188
R_m (mm)	17.4	28.5	15.6	22.2	14.2
E_i (kV/mm)	0.75	0.75	0.75	1.28	0.51
E_f (kV/mm)	0.75	2.65	0.45	1.28	0.51
V_i (kV)	14.3	38.1	11.4	23.2	9.4
Tr (%)	71	32	71	55	94

In this simple model of the cyclotron, R_m is determined by the final energy of the ion and V_d is used for maintaining the constant orbit. Thus, the free parameters left for the inflector design is only V_i, in addition to the three parameters determining the electric field of the inflector.

The injection voltage can be used to match the inflector orbit to the cyclotron orbit. In the present simple model, we assume that the tangent of the inflector central trajectory at the exit is the same as the tangent of a circle with a radius R_m, whose center lies on the center line of the acceleration gap and is off-centered so that the center of the final orbit lies on the center of the magnet. This condition determines K_i uniquely. Note, however, that in the cases of *hyperboloid* and *paraboloid* R_m determines not only the inflector electric field but also the injection voltage through $K_i = (R_m/R_0)^2$, and that no adjustable parameter is left for centering the cyclotron orbit.

Under these conditions, five examples of the inflectors are selected, all having equal path length of 60 mm through the inflector and height of 38 mm. The parameters are shown in Table I. It should be remarked that these examples are not necessarily the best solution in our situation, but they are selected in order to demonstrate the various features of the parameter selection. Since only the curvatures are relevant in the formulation, zero radius means zero curvature and negative radius negative curvature.

Transmission is defined as the percentage of number of ions transmitted through the inflector to the end without hitting the electrodes in the direction to the electric field and without deviating too much in the direction perpendicular to the electric field. The gap between the two electrodes is assumed to be 6 mm at the entrance and the width perpendicular to the electric field is 10 mm. In the simulation, 2000 ions enter the inflector along the magnetic field with 1 % velocity spread. Therefore, the results contain about a few percent of statistical error. At the entrance, the ion distribution is assumed to be circular and uniform in the transverse plane, but the position and the radial velocity are correlated to form a circular beam with a radius of 3 mm and an emittance of 200 π mm· mrad, because the ions are in the strong transverse magnetic field.

The transmissions thus calculated for the various types are shown in the bottom row of the table. The low transmission for the S6 type is reasonable because the electric field at the exit is 3.5 times stronger than at the entrance, accordingly the gap between the two electrodes are narrower as much. It is generally observed by drawing the envelope of the beam that once the ions acquire the horizontal velocity, they are converging in the median plane of the cyclotron and diverging in the direction to the magnetic field. The S6 type is disadvantageous in this respect.

The difference between the P6a and P6b types is whether the electric field helps the Lorentz force of the magnetic field or opposes it, in addition to the injection energy. P6a weakens the magnetic force and P6b strengthens it. Beam profile in the transverse plane shows that in the case of P6a, the beam seems to diverge in the direction to the electric field, where the space clearance is narrower.

4 Effects of Space Charge

In order to know the effects of the space charge of the beam on the optical properties of the inflector, let's assume the space charge force of a uniformly-charged infinitely long rod as is usually used in accelerator calculation. Since the beam diameter is of the order of a few mm and the radius of curvature of the ion motion in the inflector is more than 10 mm, this simplification is not so bad as a first order estimation. Thus we add a transverse axially symmetric electric field potential ϕ_s due to the beam with a radius r_b:

$$\frac{\phi_s}{2V_i} = \begin{cases} -f_s(r/r_b)^2 & \text{if } r < r_b \\ -f_s[\ln(r/r_b) + 1] & \text{otherwise} \end{cases} \qquad (18)$$

and

$$f_s = \frac{\rho r_b^2}{8\epsilon_0 V_i}, \qquad (19)$$

where $r = \sqrt{\xi^2 + \eta^2}$, $\rho = I/\pi r_b^2 v$ and an $^{40}\mathrm{Ar}^{10+}$ beam at the voltage V_i with current I is assumed.

The electric field produced by the inflector is of the order of $2V_iC_e$ or $2V_iC_f$, which amounts to 0.75 kV/mm in the case of model N6. On the other hand, the strength of the electric field due to the space charge is of the order of $2f_s/r_b$, which is 8.6×10^{-3} kV/mm in the case of 1

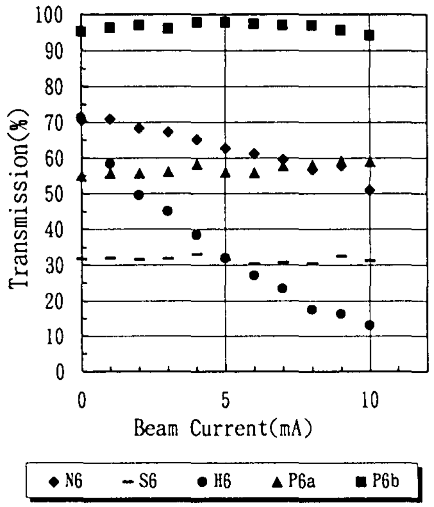

Figure 1: Beam current dependence of transmission for the selected inflector types for $^{40}Ar^{10+}$. Note that the injection voltages are different for each type of inflector as shown in the Table I.

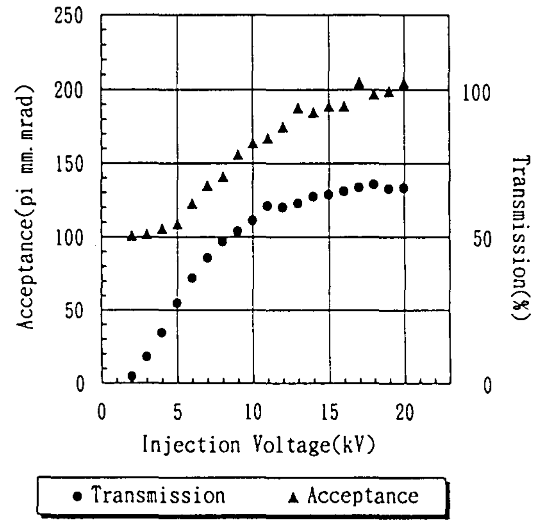

Figure 2: Injection voltage dependence of acceptance and transmission for N6 type inflector for 5 mA of $^{40}Ar^{10+}$.

mA of $^{40}Ar^{10+}$ at 10 kV for $r_b = 3$ mm and amounts to about 10 % of the external electric field at 10 mA.

The residue of the Laplacian, δ in eq.(17), naturally depends on the radii of curvature of the reference trajectory and the deviation from it, as well as the order of expansion. When we take up to 4th power in ξ or η in eqs.(15) and (16), the maximum of δ was found to be $35 \times 10^{-6} \times 2V_i$ V/mm^2 at a position 5 mm apart from the reference curve. This is equivalent to a space charge of 6.3×10^{-6} C/m^3 and to a current of 1.3 nA. Thus, the expansion is accurate enough for the present discussions.

Fig. 1 shows the beam-current dependence of the transmission for each type of the inflectors listed in Table 1. The transmissions of *parallel* and *slanted* little depend on the beam current, whereas that of *normal* decreases a little and that of *hyperboloid* does sharply with the beam current. It should be noted that since the parameters of the electric fields for these models were chosen so as to make the geometrical sizes of the inflector electrodes equal and the injection energies were determined by the centering of the orbits, the injection energies differ largely from a model to another.

Fig. 2 shows the acceptance and transmission of the N6 type inflector. The parameters for these calculations are the same as those given in Table 1, except that by varying the injection voltage for demonstration the centering condition has been omitted. The acceptance here means the rms area of the radial phase space at the entrance of those ions which are transmitted to the exit of the inflector. Since the other parameters are kept constant, the variation of the acceptance and transmission with injection voltage is purely due to the space charge.

5 Summary

The formulation of the ion motion in an electrostatic inflector enables us to overview the optical properties of various possible types of the inflectors in the uniform field approximation. At least, it guides us to design an inflector under various conditions.

Transmissions and their beam-current dependence through the space charge were found to depend strongly on the inflector types and the selection of their parameters.

In some types of inflector, the space charge affects their optical properties when the beam current exceeds a few mA for $^{40}Ar^{10+}$ at 10 kV. Conversely, if a proper type is chosen and it is designed carefully, the inflector can transmit ions up to 10 mA, at least, without deteriorating the optical properties too much.

References

1. Sekiguchi, M., Shida, Y., Ohshiro, Y., Fujita, M., Yamazaki, T., Yamazaki, N. and Nishiguchi, M., "A Formulation of Spiral Inflector Design and its Application to SF Cyclotron," Proc. 13th Int'l Conf. on Cyclotrons and their Applications, Vancouver, (World Scientific 1993) p. 450.
2. Belmont, J. L. and Pabot, J. L., "Study of Axial Injection for the Grenoble Cyclotron," IEEE Trans.Nucl.Sci., **NS-13**, 191(1966).
3. Müller, R. W., "Novel Inflectors for Cyclic Accelerators," Nucl.Instrum.Meth., **54**, 29(1967).